Paper No.
4191

CORROSION 2014
Collaborate. Educate. Innovate. Mitigate.
March 9-13, 2014 • Henry B. Gonzalez Convention Center • San Antonio, Texas, U.S.A.

Study of the Catalytic Behavior of H_2S on the Corrosion of High Strength Carbon Steel in Deaerated Marine Environments

Justin Beck
Department of Energy and Mineral Engineering
Pennsylvania State University
University Park, PA 16802
USA

Serguei Lvov
Department of Energy and Mineral Engineering
Pennsylvania State University
University Park, PA 16802
USA

Ruishu Feng
Department of Energy and Mineral Engineering
Pennsylvania State University
University Park, PA 16802
USA

Margaret Ziomek-Moroz
National Energy Technology Laboratory
1450 Queen Avenue SW
Albany, OR 97321
USA

ABSTRACT

Electrochemical investigations were performed for corrosion of high strength low alloy carbon steel in neutral and basic brine solutions at temperatures around 30 °C. Thermodynamic modeling at these conditions predicted that HS^- would be the dominant species for dissolved H_2S at basic pH and would increase in concentration at constant H_2S partial pressure with increasing pH. Undissociated H_2S was predicted to increase in concentration with increasing solution temperature, but was not expected to vary greatly with solution pH. Initial measurements using impedance spectroscopy after 60 hours of exposure found that while the impedance magnitude increased with decreasing sulfide concentration and increasing solution pH, the phase angle behavior was relatively unchanged. There was a significant shift in the high frequency phase angle when sulfide-free solution was tested. When the rate of stirring was decreased, LPR slopes for the cathodic polarization remained unchanged for sulfide-containing solutions but increased in slope for sulfide-free solution. Initial results suggest that the presence of dissolved H_2S may affect the cathodic reaction mechanism beyond simply reducing the solution pH.

Key words: H_2S corrosion; neutral and basic pH; electrochemical impedance spectroscopy; linear polarization resistance; high strength low alloy steel

INTRODUCTION

The effects of hydrogen sulfide (H_2S) on the corrosion of high strength low alloy (HSLA) carbon steel have been well studied due to their relevance to the oil and natural gas industries. Since H_2S behaves as an acid in aqueous solutions, the presence of dissolved H_2S results in a decrease in pH through

©2014 by NACE International.
Requests for permission to publish this manuscript in any form, in part or in whole, must be in writing to
NACE International, Publications Division, 1440 South Creek Drive, Houston, Texas 77084.
The material presented and the views expressed in this paper are solely those of the author(s) and are not necessarily endorsed by the Association.

dissociation into H^+ and HS^- ions. The effects of sulfide on iron oxidation have been found to be dependent on the solution pH. At very low pH the metal surface has been found to be free of corrosion products, which results in high rates of active corrosion.[1–3] As the pH increases in the range of 3 to 5, the addition of H_2S has been found to result in an initial increase in corrosion rate that decreases over time as a protective iron sulfide layer forms over the metal surface.[2,4–6] Mackinawite was generally observed to form as the initial corrosion product. Over time this layer could convert to more protective films of troilite, pyrrhotite, and pyrite.

While the formation of sulfide films has been found to decrease the overall rate of corrosion, defects in the resulting passive layers often shifts the corrosion from uniform to localized in nature.[3,6,7] Such localized pitting and crevice corrosion can render steels more susceptible to stress corrosion cracking (SCC), hydrogen induced cracking (HIC), and corrosion fatigue (CF). The particularly susceptibility caused by sulfides has resulted in a specific condition of sulfide stress cracking (SSC), or sulfide stress corrosion cracking (SSCC), which has also been well studied over the years.[8–10] However, while the corrosion and cracking behavior of HSLA steels in acidic solutions containing sulfides have been given great attention there is considerably less information available for behavior in neutral and basic conditions.

Recently, work was performed to study cracking of steel under cyclic stress in solutions from pH 7 to 12.[11,12] Their results found cracking to be controlled by hydrogen diffusion for CF at pH 7, whereas it was more representative of SCC at pH 12. A transition in behavior was observed at pH 9 between H_2S partial pressures of 0.12 psi (0.827 kPa) and 1.2 psi (8.27 kPa). The purpose of the work described here was to perform an initial investigation of the corrosion behavior of ultrahigh strength low alloy steel in sulfide solutions of neutral and basic pH in order to better understand the mechanisms leading to this changeover in cracking behavior from CF to SCC.

THERMODYNAMIC MODELING OF SPECIATION

In order to understand the possible mechanisms involved in sulfide corrosion, the reacting species must be considered. Many of the works cited in the previous section proposed mechanisms in acidic conditions where undissociated H_2S reacts directly with the active steel to produce iron sulfides through an Fe-HS^- intermediate. If this mechanism is prevalent in neutral and basic solutions, then it should be understood how changing solution pH and temperature would be expected to affect the corrosion process through changing H_2S solubility and speciation. Thermodynamic modeling was performed for predicting the speciation of H_2S in aqueous solutions with 5 %wt. NaCl and the effect of pH on H_2S as a function of temperature and H_2S partial pressure. The calculations presented here were performed using the HCh[(†)] chemical simulation software.[13] It was chosen because it allows speciation calculations to be performed assuming a gas phase with a given pressure.

The results for calculations performed at 25 °C are shown in Figures 1 and 2. Changes in solution pH were modeled using varying concentrations of HCl and NaOH. In all cases the predominant species were dissolved H_2S and its dissociation into HS^-. Further dissociation into S^{2-} was found to be unfavorable, which has been well documented in previous studies for H_2S-water and H_2S-water-salt systems.[14,15] It can be seen that the concentration of H_2S is expected to depend greatly on partial pressure, but little variation is seen with pH. The concentration of HS^- is expected to increase with both increasing H_2S partial pressure and solution pH.

[†] Trade name.

©2014 by NACE International.
Requests for permission to publish this manuscript in any form, in part or in whole, must be in writing to
NACE International, Publications Division, 1440 South Creek Drive, Houston, Texas 77084.
The material presented and the views expressed in this paper are solely those of the author(s) and are not necessarily endorsed by the Association.

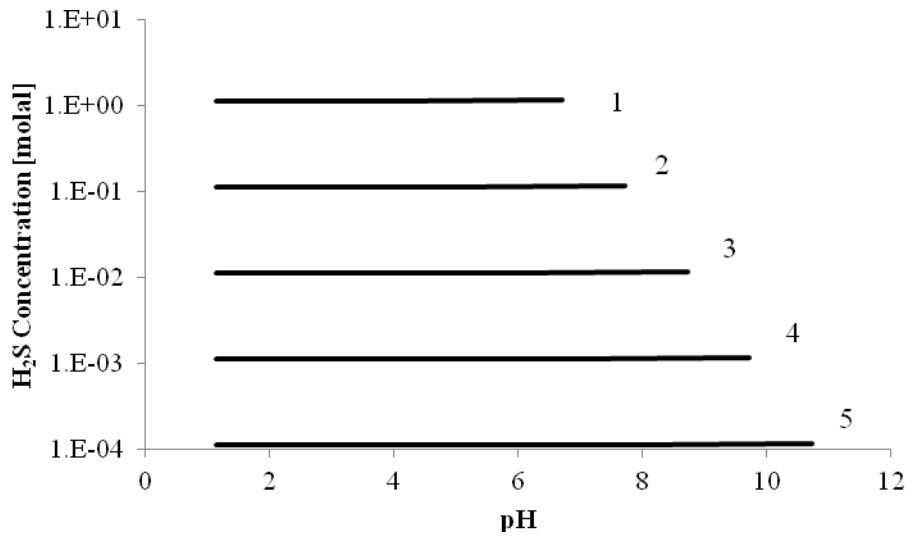

Figure 1: Thermodynamic modeling of dissolved H_2S molal concentration at 25 °C as a function of solution pH and H_2S partial pressure; 1 = 1.0 MPa, 2 = 0.1 MPa, 3 = 10 kPa, 4 = 1.0 kPa, and 5 = 0.1 kPa.

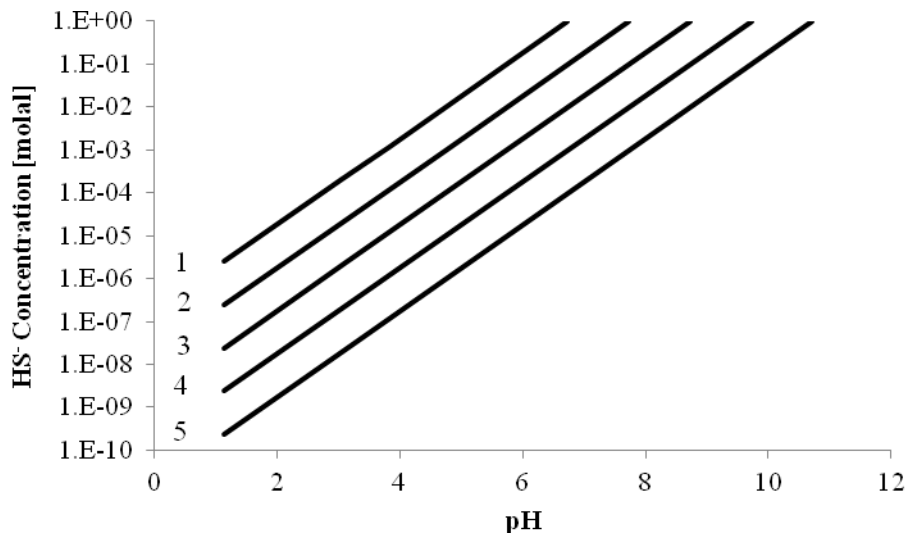

Figure 2: Thermodynamic modeling of dissolved HS^- molal concentration at 25 °C as a function of solution pH and H_2S partial pressure; 1 = 1.0 MPa, 2 = 0.1 MPa, 3 = 10 kPa, 4 = 1.0 kPa, and 5 = 0.1 kPa.

The effect of temperature on H_2S concentration for 1.0 kPa H_2S from 25 to 200 °C are shown in Figure 3. Gases generally have reduced solubility with increasing temperature, and this is readily observed in the figure. However, it can also be seen that the concentration reaches a minimum around 0.3 to 0.4 mmol kg^{-1} H_2S between 100 and 200 °C. A similar analysis for HS^- concentration found almost no change with respect to temperature, showing that HS^- is expected to only be a function of solution pH and H_2S partial pressure, whereas dissolved H_2S is expected to vary with H_2S partial pressure and temperature, though the effect is less dramatic as the temperature increases above 100 °C.

©2014 by NACE International.
Requests for permission to publish this manuscript in any form, in part or in whole, must be in writing to
NACE International, Publications Division, 1440 South Creek Drive, Houston, Texas 77084.
The material presented and the views expressed in this paper are solely those of the author(s) and are not necessarily endorsed by the Association.

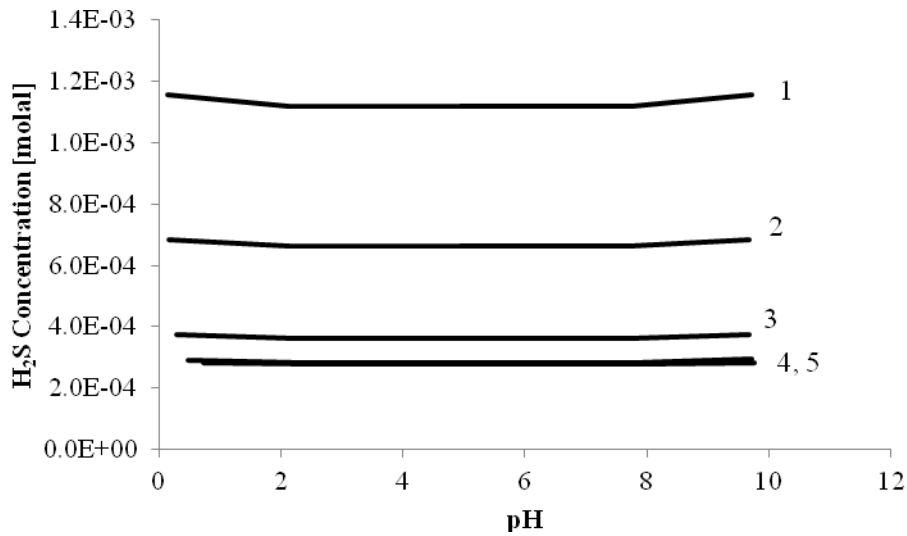

Figure 3: Thermodynamic modeling of dissolved H_2S molal concentration at 0.01 psi (69 Pa) H_2S as a function of solution pH and temperature; 1 = 25 °C, 2 = 50 °C, 3 = 100 °C, 4 = 150 °C, and 5 = 200 °C.

These results allow us to begin preparing hypotheses for the effects of changing environments on sulfide-based corrosion mechanisms. If the corrosion process is largely dependent on the concentration of dissolved H_2S, as has been proposed elsewhere for acidic solutions, then increasing temperature would reduce the concentration and result in a significant decrease in the corrosion rate. Little or no change would be expected due to changing solution pH. If the concentration of HS^- dictates the overall corrosion rate, then the opposite behavior would be observed. Increasing pH would greatly increase the corrosion rate, while changing temperature should have little effect. In both cases increasing the partial pressure of H_2S should increase the corrosion rate.

EXPERIMENTAL PROCEDURE

Experimental System

The experimental system was designed to allow for electrochemical measurements to be performed using a three electrode cell in a well-stirred reactor vessel. The working electrode consisted of a 1 x 2 x 0.5 cm planar sample made of UNS G41300 HSLA steel drill pipe meeting API grade S135. The chemical composition of the HSLA steel is shown in Table 1.

TABLE 1. Chemical Composition [%wt.] of UNS G41300

Fe	Cr	Mn	Mo	Al	Ni	Cu	Nb	S	P	B	C	N
Bal	1.39	0.78	0.68	0.03	0.02	0.02	<0.01	0.002	0.006	<0.005	0.26	0.005

The samples were coated with a bisphenol-amine epoxy so that only the 10 x 20 mm face opposite the counter electrode was exposed to solution. The counter electrode was a 10 x 20 x 1 mm platinum plate. Figure 4a shows the electrode assembly. The two electrodes were held in place between two polytetrafluoroethylene (PTFE) plates. Pressure was applied by tightening two PTFE-coated screws threaded into the PTFE plates. A hole has been drilled through the top PTFE plate to allow positioning of the reference electrode tip between the working and counter electrodes without obscuring the path for ion transport.

©2014 by NACE International.
Requests for permission to publish this manuscript in any form, in part or in whole, must be in writing to
NACE International, Publications Division, 1440 South Creek Drive, Houston, Texas 77084.
The material presented and the views expressed in this paper are solely those of the author(s) and are not necessarily endorsed by the Association.

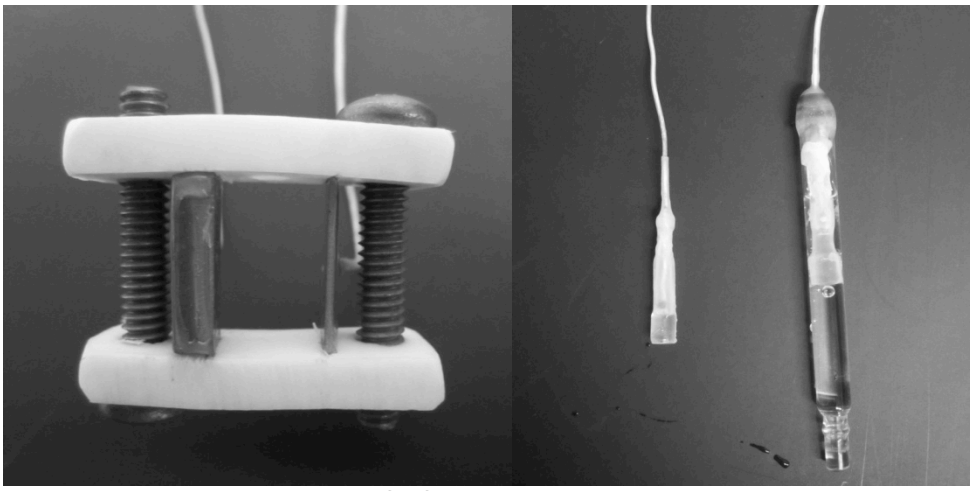

Figure 4: a) The electrode assembly (left) for the working and counter electrodes; b) the inner and outer junctions (right) for the double junction reference electrode.

The reference electrode was a double junction silver-silver chloride (Ag/AgCl) electrode as shown in Figure 4b. A fill solution of 5 %wt. NaCl was chosen to minimize the chloride concentration gradient, and thus the junction potential, between the reference electrode and the test solutions to improve the measurement accuracy. Use of the silver-silver sulfide (Ag/Ag_2S) couple was considered for the reference electrode to prevent effects from sulfide contaminations of the reference solutions. However, sulfide electrodes have been reported to have had difficulty in providing thermodynamically predictable potentials, which was desired here in order to perform thermodynamic analysis for future tests.[16] Additionally, Crowe and Tromans have reported issues with thermodynamic potential predictions as the solution temperature increases.[17] Thus, a decision was made to use the more thermodynamically predictable Ag/AgCl couple with well-controlled diffusion junctions to prevent solution contamination over the test period. The reference electrode was inserted into a PTFE tube filled with NaCl solution. The top of the tube was sealed with epoxy, while the bottom junction was fitted with a porous glass frit. This inner assembly was inserted into a glass tube, which was filled with the same NaCl reference solution. The top was again sealed with epoxy, while the bottom contained a second glass frit to form the junction with the test solution. Initial system tests in a solution prepared using a diluted H_2S-saturated stock solution found the double junction electrode to be very stable, with only a 2 to 3 mV drift in potential observed after a five day exposure in H_2S solution at 30 °C when measured against a commercial reference electrode before and after exposure.

A 600 ml stirred autoclave vessel was chosen as the reactor vessel to allow for pressurized operation for the 200 °C measurements. The vessel was constructed of UNS S31600 stainless steel, and a PTFE liner was used to prevent contamination of the test solution from any corrosion products that could result from reaction of the autoclave vessel. The autoclave lid, shown on the left of Figure 5a, was used to mount a pressure gage, pressure transducer, and thermocouple. A polymer-coated thermocouple was selected to prevent corrosion damage of the sensor and possible contamination of the test solution with undesired corrosion products. The stirrer was also coated with epoxy to prevent undesired corrosion. The electrode leads were sealed using a PTFE compression gland fitted to the lid.

©2014 by NACE International.
Requests for permission to publish this manuscript in any form, in part or in whole, must be in writing to
NACE International, Publications Division, 1440 South Creek Drive, Houston, Texas 77084.
The material presented and the views expressed in this paper are solely those of the author(s) and are not necessarily endorsed by the Association.

Figure 5: a) Autoclave vessel, liner and lid assembly (left); b) assembled system (right) with, from left to right: computer-controlled potentiostat, autoclave system with stirrer and heating mantle, and autoclave controller.

Figure 5b shows the assembled system. The autoclave controller was connected to a computer to allow recording of the system temperature and pressure over the course of the exposure. A computer-controlled potentiostat was used to perform linear polarization resistance (LPR), electrochemical frequency modulation (EFM), and electrochemical impedance spectroscopy (EIS) measurements to investigate the corrosion behavior in real-time. The test system was been placed inside a protective enclosure to reduce the risk to personnel in the event of autoclave leak or failure.

Experimental Procedure

The H_2S was supplied by a stock solution of water saturated with 100 kPa H_2S at 25 °C. The autoclave vessel was held at 30 or 35 °C and ambient pressure over the course of the exposure. Three solutions were tested. In the first two solutions, the stock H_2S solution was diluted with deaerated distilled water in a glove bag under argon. Sodium chloride was added for a concentration of 5 %wt., and the solution was buffered with a measured amount of Na_2CO_3. The third solution contained deaerated distilled water with 5 %wt. NaCl and 0.5 mol kg^{-1} $NaHCO_3$, but no H_2S was added.

Measurements of solution pH before the autoclave was assembled were used to calculate the total sulfide concentration. Calculations were performed using OLI Analyzer(†) modeling software.[18] The solution for the first sample had a pH of 6.91 after the addition of 3.88 mmol kg^{-1} Na_2CO_3, which corresponded to a sulfide concentration of 6.57 mmol kg^{-1}. The second sample solution had a pH of 8.51 after addition of the same amount of Na_2CO_3, corresponding to a sulfide concentration of 3.61 mmol kg^{-1}. The third solution had a final pH of 7.62 after buffering with 0.5 mol kg^{-1} $NaHCO_3$.

Once the test solution was prepared, the autoclave vessel was assembled under argon. The test vessel was then brought to a stable temperature, after which the electrochemical measurements were begun. The first test at neutral pH was held at ambient conditions, which at the time was 30 °C and fluctuated by up to 3 °C. The second two tests were conducted at 35 °C to provide more

† Trade name.

©2014 by NACE International.
Requests for permission to publish this manuscript in any form, in part or in whole, must be in writing to
NACE International, Publications Division, 1440 South Creek Drive, Houston, Texas 77084.
The material presented and the views expressed in this paper are solely those of the author(s) and are not necessarily endorsed by the Association.

stable temperature control over the exposure period, and temperature was maintained within 1 °C. Electrochemical impedance spectroscopy (EIS) and linear polarization resistance (LPR) measurements were performed over 60 hours of exposure.

RESULTS

For all EIS measurements, two time-constants were observed over the frequency range from 1 kHz down to 1 mHz. The Nyquist plots are shown in Figure 6, and the phase angle data are shown in Figure 7. For the two tests with H_2S, the phase angle peaks occurred at about 1 Hz and 10 mHz. However, when no H_2S was present the higher frequency phase angle peak shifted up to around 10 Hz. Additionally, the lower frequency phase angle peak had a larger magnitude than the lower frequency peak, whereas the higher frequency peak was larger for the solution without H_2S. This could suggest a change in reaction mechanism when H_2S is present in the solution.

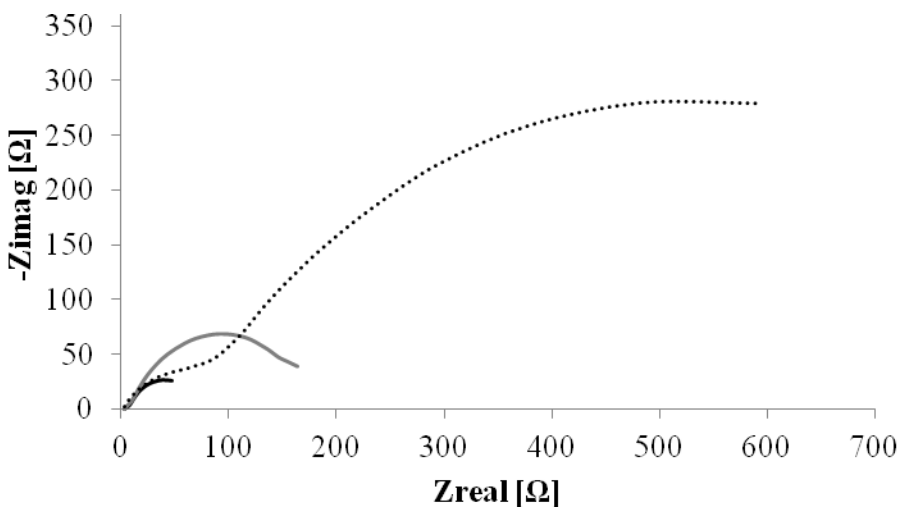

Figure 6: Nyquist plot for EIS measurements at 60 hours of exposure; black and grey solid lines are results for H_2S samples 1 and 2, dotted black line is for H_2S-free solution.

This shift in behavior would be expected if the anodic reaction, which is the oxidation of iron, is the rate limiting step in the corrosion reaction. However, in many corrosion systems the overall reaction rate is often limited by mass transport for the cathodic reaction. This is one of the reasons why reducing the solution pH can result in a significant increase in corrosion rate, as it means that the concentration of H^+ ions has been increased to boost the hydrogen evolution kinetics. If the cathodic reaction was the rate limiting step for this system, these results would suggest that in neutral and basic solutions dissolved H_2S and HS^- could be directly involved in the cathodic reduction reaction. It appears that the change in mechanism would correspond to the higher frequency time constant, since the lower frequency time constant did not shift significantly.

©2014 by NACE International.
Requests for permission to publish this manuscript in any form, in part or in whole, must be in writing to
NACE International, Publications Division, 1440 South Creek Drive, Houston, Texas 77084.
The material presented and the views expressed in this paper are solely those of the author(s) and are not necessarily endorsed by the Association.

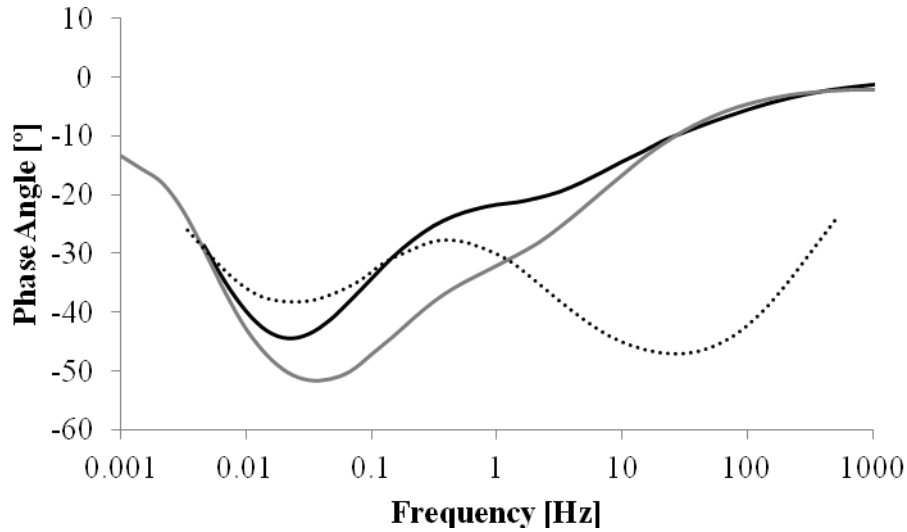

Figure 7: Bode plot for EIS measurements at 60 hours of exposure; black and grey solid lines are results for H_2S samples 1 and 2, dotted black line is for H_2S-free solution.

In order to better understand the nature of any mass transport limitations, measurements were also performed at a reduced stirring rate once steady-state behavior was reached. Figure 8 shows the LPR data for a 10 mV sweep around the corrosion potential for one of the UNS G41300 steel samples exposed to H_2S. For both H_2S-exposed tests the same trends were observed: the cathodic slope saw a negligible change as the stirring rate was reduced, while a significant increase was seen in the anodic slope. This appears to suggest two properties of the H_2S corrosion mechanism. First, the lack of effect of stirring on the cathodic slope would mean that the process was not diffusion limited. If mass transport was in any way limiting the cathodic corrosion rate, it would have been likely due to some chemical process preceding the electrochemical charge transfer step, such as the adsorption of an intermediate species. Second, for the anodic process it would normally be expected for the corrosion rate to increase as stir rate also increases. Since the LPR slope as presented in Figure 8 is inversely proportional to the polarization resistance, increased stirring would result in an increase in slope and thus an increase in the rate of corrosion. However, the observation of the opposite trend here would suggest that increasing the rate of stirring must actually have removed some active species from the electrode surface. This could mean that the anode reaction is limited to some extent by the concentration of an intermediate species not present in the bulk solution.

Figure 9 shows the LPR results for the solution without H_2S, where it can be seen that both the anodic and cathodic slopes were affected by the stirring rates. For both processes it was observed that decreasing the rate of stirring decreased the polarization resistance, which would correspond to an increase in corrosion rate. The change in cathodic behavior again suggests that the presence of H_2S changes the reduction mechanism. The EIS results for the H_2S solutions saw an increase in the low-frequency impedance as the stirring rate was reduced, which would be expected to correspond to a decrease in the limiting current. A slight decrease was observed in the phase angle peak with reduced rate of stirring, and the peak shifted to a slightly lower frequency. The H_2S-free solution results are shown in Figures 10 and 11. It can be seen in the Nyquist plot that decreasing the rate of stirring resulted in a large increase in the impedance of the higher frequency time constant. The phase angle data showed a shift to higher frequency for the higher frequency phase angle, while the lower frequency peak shifted to an even lower potential. While the significance of this behavior has not yet

©2014 by NACE International.
Requests for permission to publish this manuscript in any form, in part or in whole, must be in writing to
NACE International, Publications Division, 1440 South Creek Drive, Houston, Texas 77084.
The material presented and the views expressed in this paper are solely those of the author(s) and are not necessarily endorsed by the Association.

been determined, it should be noted that the deviation in behavior from the samples exposed to H_2S suggests that the limiting step for the sulfide corrosion mechanism differs in neutral and basic solutions.

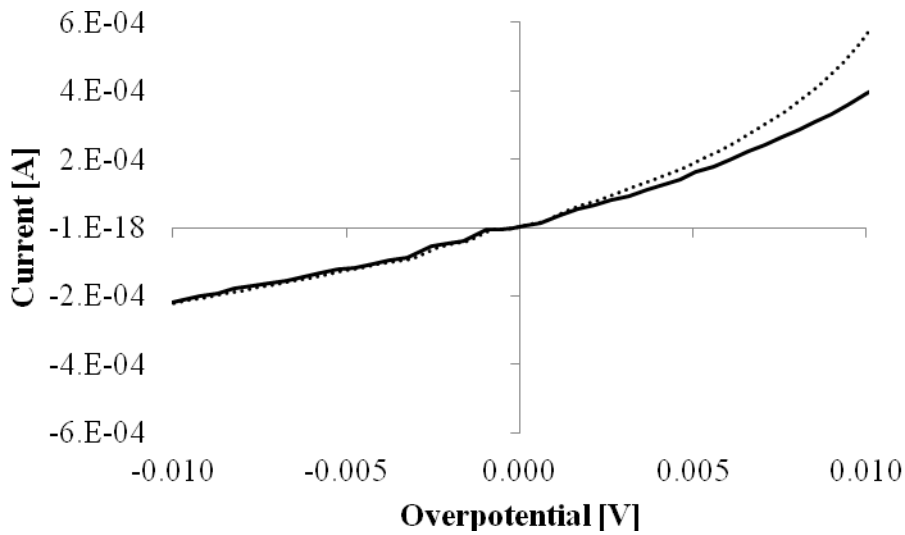

Figure 8: LPR data for sample exposed to solution with H_2S; solid line = higher stirring rate, dotted line = lower stirring rate.

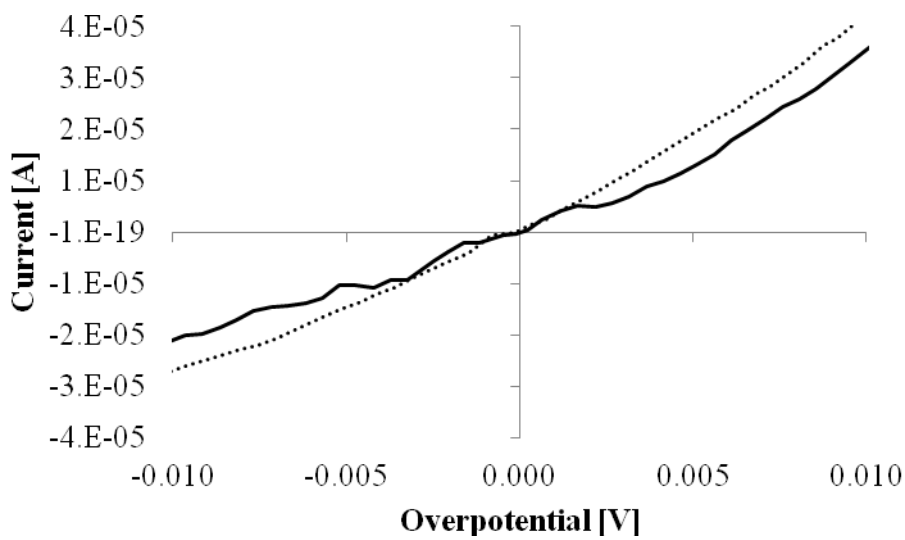

Figure 9: LPR data for sample exposed to solution without H_2S; solid line = higher stirring rate, dotted line = lower stirring rate.

©2014 by NACE International.
Requests for permission to publish this manuscript in any form, in part or in whole, must be in writing to
NACE International, Publications Division, 1440 South Creek Drive, Houston, Texas 77084.
The material presented and the views expressed in this paper are solely those of the author(s) and are not necessarily endorsed by the Association.

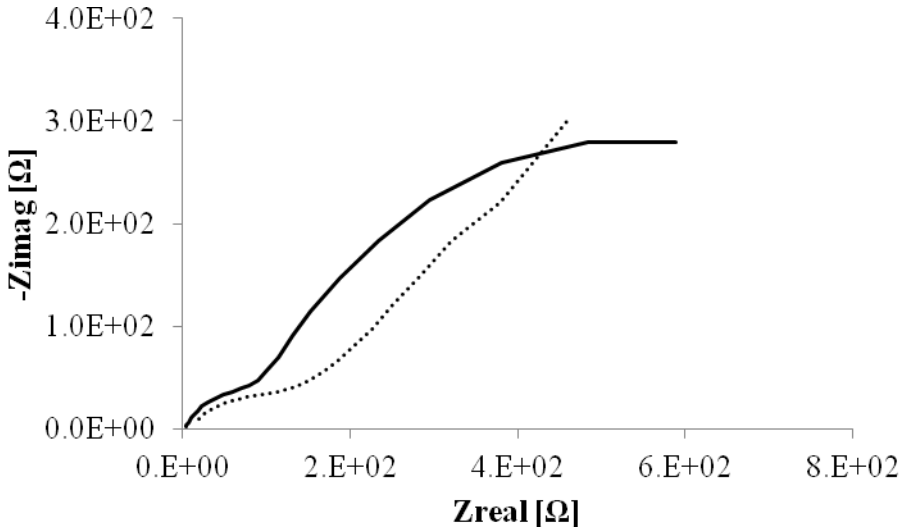

Figure 10: Nyquist plot for sample exposed to solution without H_2S; solid line = higher stirring rate, dotted line = lower stirring rate.

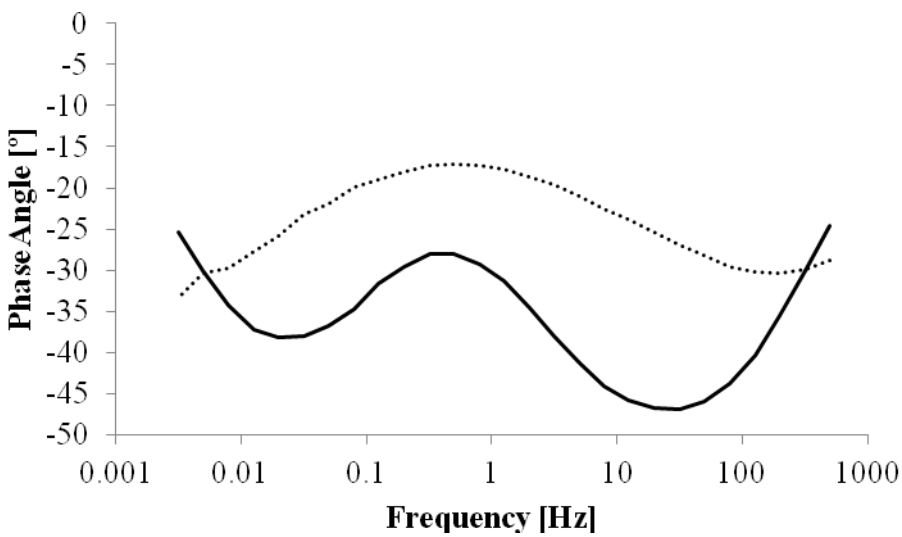

Figure 11: Bode plot for sample exposed to solution without H_2S; solid line = higher stirring rate, dotted line = lower stirring rate.

When conducting any investigation of reaction mechanism it is important to consider the rate limiting step of the overall process. Electrochemical measurements directly observe the rate of the charge transfer step by measuring the current response of a potential perturbation. Since every electrochemical system involves both an oxidation and reduction process, it would not be unexpected that either the anodic or cathodic process be more kinetically limiting than the other. As was previously mentioned, many corrosion systems are cathodically limited due to mass transport of some active species to the electrode surface. Since the anode process consumes the active metal that served as the anode, there is little expectation of mass transport limits. In aerated solutions cathodic mass transport limits can be due to the low solubility of oxygen in aqueous solutions, and it was already mentioned how decreasing the solution pH can significantly increase corrosion rates by increasing the concentration of H^+ ions.

©2014 by NACE International.
Requests for permission to publish this manuscript in any form, in part or in whole, must be in writing to
NACE International, Publications Division, 1440 South Creek Drive, Houston, Texas 77084.
The material presented and the views expressed in this paper are solely those of the author(s) and are not necessarily endorsed by the Association.

One of the issues when performing corrosion measurements at the corrosion potential is that, while it provides the most accurate representation of the corrosion behavior at that condition, it is not always obvious which process, anodic or cathodic, is being observed as the rate limiting step. For this reason it can become necessary to perform measurements such as EIS at polarized conditions. This can ensure that the observed behavior is specifically anodic or cathodic in nature. Ma et al. have previously performed such measurements at anodic polarizations for steel in neutral H_2S solutions.[19] Their results showed a significant change in EIS behavior between measurements at the corrosion potential and at anodic polarizations. Large polarizations saw further changes in the behavior, with the two time constants previously observed shrinking to a single time constant.

In order to further investigate the anodic corrosion mechanism for steels exposed to H_2S we are preparing additional measurements to be performed with fixed H_2S pressures to better control the concentration of sulfide species in solution. Measurements will be performed at the corrosion potential, as well as anodic polarizations, for solutions with neutral to basic pH. Our goal will be to better characterize the change in sulfide assisted fatigue crack propagation behavior reported by Ramgopal et al. between pH 7 and 9 and H_2S pressures of 0.12 and 1.2 psi (0.827 and 8.27 kPa).[12]

CONCLUSIONS

It has been shown that while decreasing the concentration of H_2S resulted in an increase in the impedance of the low frequency time constant, the difference was not as large as that observed when no H_2S was present. Additionally, the presence of H_2S shifted the peak of the phase angle for the higher frequency time constant to a lower frequency, though it did not affect the lower frequency phase angle. LPR results showed that decreasing the rate of stirring decreased the polarization resistance for both the anodic and cathodic processes for solution without H_2S, but only affected the anodic slope when H_2S was added to solution. Decreasing the stir rate increased the impedance of the low frequency time constant for all cases, but a significant shift in both of the phase angle peaks was also observed for the sample exposed to H_2S-free solution. Our future mechanism investigations will include additional measurements at polarized conditions to better understand the rate limiting processes and the anodic reaction mechanism.

DISCLAIMER

This report was prepared as an account of work sponsored by an agency of the United States Government. Neither the United States Government nor any agency thereof, nor any of their employees, makes any warranty, express or implied, or assumes any legal liability or responsibility for the accuracy, completeness, or usefulness of any information, apparatus, product, or process disclosed, or represents that its use would not infringe privately owned rights. Reference herein to any specific commercial product, process, or service by trade name, trademark, manufacturer, or otherwise does not necessarily constitute or imply its endorsement, recommendation, or favoring by the United States Government or any agency thereof. The views and opinions of authors expressed herein do not necessarily state or reflect those of the United States Government or any agency thereof.

REFERENCES

1. Shoesmith, D. W., Taylor, P., Bailey, M. G., and Owen, D. G. “The Formation of Ferrous Monosulfide Polymorphs during the Corrosion of Iron by Aqueous Hydrogen Sulfide at 21°C,” *Journal of The Electrochemical Society* **127** (1980): 1007.

©2014 by NACE International.
Requests for permission to publish this manuscript in any form, in part or in whole, must be in writing to
NACE International, Publications Division, 1440 South Creek Drive, Houston, Texas 77084.
The material presented and the views expressed in this paper are solely those of the author(s) and are not necessarily endorsed by the Association.

2. Ma, H., Cheng, X. L., Chen, S. H., Li, G. Q., Chen, X., Lei, S. B., and Yang, H. Q. "The influence of hydrogen sulfide on corrosion of iron under different conditions," *Corrosion Science* **42** (2000): 1669–1683.

3. Tang, J., Shao, Y., Zhang, T., Meng, G., and Wang, F. "Corrosion behaviour of carbon steel in different concentrations of HCl solutions containing H2S at 90°C," *Corrosion Science* **53** (2011): 1715–1723.

4. Huang, H., Tsai, W., and Lee, J. "Electrochemical Behavior of A516 Carbon Steel in Solutions Containing Hydrogen Sulfide," *Corrosion* **52** (1996): 708–713.

5. El Mendili, Y., Abdelouas, A., and Bardeau, J.-F. "Impact of a sulphidogenic environment on the corrosion behavior of carbon steel at 90 °C," *RSC Advances* **3** (2013): 15148-15156.

6. Ren, C., Liu, D., Bai, Z., and Li, T. "Corrosion behavior of oil tube steel in simulant solution with hydrogen sulfide and carbon dioxide," *Materials Chemistry and Physics* **93** (2005): 305–309.

7. Videm, K. and Kvarekvål, J. "Corrosion of Carbon Steel in Carbon Dioxide-Saturated Solutions Containing Small Amounts of Hydrogen Sulfide," *Corrosion* **51** (1995): 260–269.

8. Treseder, R. S. and Swanson, T. M. "Factors in Sulfide Corrosion Cracking of High Strength Steels," *Corrosion* **24** (1968): 31–37.

9. Kimura, M., Totsuka, N., Kurisu, T., Amano, K., Matsuyama, J., and Nakai, Y. "Sulfide Stress Corrosion Cracking of Line Pipe," *Corrosion* **45** (1989): 340–346.

10. Carneiro, R. A., Ratnapuli, R. C., and de Freitas Cunha Lins, V. "The influence of chemical composition and microstructure of API linepipe steels on hydrogen induced cracking and sulfide stress corrosion cracking," *Materials Science and Engineering: A* **357** (2003): 104–110.

11. Ziomek-Moroz, M., Hawk, J. A., Thodla, R., and Gui, F. "Effect of Sour Environment pH on Crack Morphology in Ultra-High Strength Drilling Steel Under Cyclic Stress," *ECS Transactions* **50** (2013): 79–90.

12. Ramgopal, T., Gui, F., Hawk, J., and Ziomek-Moroz, M. "Corrosion Fatigue Performance of High Strength Drill Pipe In Sour Environments," *CORROSION 2011*, paper no. 165 (Houston, TX: NACE 2011)**,** 1–11.

13. Shvarov, Y. V. "Algorithmization of the Numeric Equilibrium Modeling of Dynamic Geochemical Processes," *Geochemistry International* **37** (1999): 571–576.

14. Millero, F. J. "The thermodynamics and kinetics of the hydrogen sulfide system in natural waters," *Marine Chemistry* **18** (1986): 121–147.

15. Morse, J., Millero, F., Cornwell, J., and Rickard, D. "The chemistry of the hydrogen sulfide and iron sulfide systems in natural waters," *Earth-Science Reviews* **24** (1987): 1–42.

16. Ives, D.J.G. and Janz, G.J. *Reference Electrodes: Theory and Practice*, First Edition (New York City, New York: Academic Press, 1961).

©2014 by NACE International.
Requests for permission to publish this manuscript in any form, in part or in whole, must be in writing to
NACE International, Publications Division, 1440 South Creek Drive, Houston, Texas 77084.
The material presented and the views expressed in this paper are solely those of the author(s) and are not necessarily endorsed by the Association.

17. Crowe, D.C. and Tromans, D. “The Silver Sulfide Reference Electrode for use in Alkaline Sulfide Solutions,” *CORROSION* **42** (1986): 409-415.

18. OLI Systems, Inc. “Analyzer Studio 9,” (2013).

19. Ma, H. Y., Cheng, X. L., Chen, S. H., Li, G. Q., Chen, X., Lei, S. B., and Yang, H. Q. “Theoretical Interpretation on Impedance Spectra for Anodic Iron Dissolution in Acidic Solutions Containing Hydrogen Sulfide,” *Corrosion* **54** (1998): 634–640.

©2014 by NACE International.
Requests for permission to publish this manuscript in any form, in part or in whole, must be in writing to
NACE International, Publications Division, 1440 South Creek Drive, Houston, Texas 77084.
The material presented and the views expressed in this paper are solely those of the author(s) and are not necessarily endorsed by the Association.